Journal of Hazardous Materials Letters 3 (2022) 100054

Contents lists available at ScienceDirect

Journal of Hazardous Materials Letters

journal homepage: www.sciencedirect.com/journal/journal-of-hazardous-materials-letters

Degradation of 1,4-dioxane by reactive species generated during breakpoint chlorination: Proposed mechanisms and implications for water treatment and reuse☆

Samuel D. Patton [a], Michael C. Dodd [b,*], Haizhou Liu [a,c,**]

[a] Environmental Toxicology Program, University of California, Riverside, CA 92521, USA
[b] Department of Civil and Environmental Engineering, University of Washington, Seattle, WA 98195, USA
[c] Department of Chemical and Environmental Engineering, University of California, Riverside, CA 92521, USA

ARTICLE INFO

Keywords:
Breakpoint chlorination
Reactive species
Peroxynitrite
Hydroxyl radical
1,4-dioxane

ABSTRACT

Breakpoint chlorination, an important chemical process relevant to chlorine-based advanced oxidation processes for potable reuse and to traditional water treatment, was investigated for its oxidative capacity, generation of reactive species, and potential impacts on organic contaminant degradation. This work describes a newly recognized $HO^{\bullet}$ radical generation pathway during breakpoint chlorination that may play an important role in water treatment and examines the behavior of the $HO^{\bullet}$ radical and other related reactive species and their potential formation pathways. Experimental data showed that the removal of 1,4-dioxane (1,4-D) positively correlated with chlorine-to-ammonia molar ratio until a molar ratio of ~1.5–2.0 was reached, above which removal efficiency rapidly decreased. Peroxynitrite ($ONOO^-$) and peroxynitrous acid (ONOOH) are proposed as important radical sources that lead to the formation of $HO^{\bullet}$ in the breakpoint process. This is supported by application of *tert*-butanol as a selective $HO^{\bullet}$ scavenger and the observation that the amendment of reaction solutions with carbonate species suppressed oxidative capacity to a much greater extent than expected based solely on scavenging of $HO^{\bullet}$ by H_2CO_3 * /CO_2 and HCO_3^- (apparently due to selective scavenging of ONOOH/$ONOO^-$ by dissolved CO_2). These experiments also provided evidence that reactive species other than $HO^{\bullet}$ contributed to 1,4-D oxidation. The results of this study suggest that breakpoint chlorination can lead to significant degradation of organic contaminants via ONOOH/$ONOO^-$-mediated formation of $HO^{\bullet}$ and other reactive species and may potentially be optimized for enhanced removal of recalcitrant organic contaminants in the context of water reuse, though with due caution to the potential for enhancement of nitrogenous and other disinfection byproduct formation under such conditions.

1. Introduction

Free chlorine has long been used as a disinfectant and oxidant in water treatment, both for inactivating pathogens and for oxidizing certain contaminants. In recent years, free chlorine photolysis has been examined as a promising advanced oxidation process (AOP) for removing trace organic contaminants from reverse osmosis (RO) permeate for potable reuse, and full-scale implementation is under consideration by many water agencies (Zhang et al., 2018; Remucal and Manley, 2016; Duan et al., 2018). However, some critical aspects of chlorine chemistry in recycled water and general treatment remain incompletely understood, especially regarding the effects of nitrogen species (e.g., ammonia) in wastewater effluent and potable water supplies. Ammonia is ubiquitous in municipal wastewaters and frequently present in reduced groundwaters. Consequently, the addition of free chlorine in such systems needs to overcome the chlorine breakpoint to produce residual chlorine for AOP application or conventional treatment.

Breakpoint chlorination refers to the chemical processes occurring when free chlorine is applied to ammonia-containing waters. Upon contact with ammonia, free chlorine produces a mixture of chloramines, including monochloramine (NH_2Cl), dichloramine ($NHCl_2$) and

☆ Submitted to Journal of Hazardous Materials Letters

* Corresponding author.
** Correspondence to: Department of Chemical and Environmental Engineering, Riverside, CA 92521, USA.
E-mail addresses: doddm@uw.edu (M.C. Dodd), haizhou@engr.ucr.edu (H. Liu).

https://doi.org/10.1016/j.hazl.2022.100054
Received 23 December 2021; Received in revised form 1 April 2022; Accepted 29 April 2022
Available online 4 May 2022

trichloramine (NCl_3), depending on molar ratio of free chlorine to ammonia and pH (R1 – R3):(Vikesland et al., 2001)

$$NH_3 + HOCl \rightarrow NH_2Cl + H_2O \quad (R1)$$

$$NH_2Cl + HOCl \rightarrow NHCl_2 + H_2O \quad (R2)$$

$$NHCl_2 + HOCl \rightarrow NCl_3 + H_2O \quad (R3)$$

At pH 7, and when other significant chlorine sinks are absent, theoretical breakpoint occurs at the chlorine-to-ammonia molar ratio of 1.5, where ammonia becomes nitrogen gas and the free chlorine is reduced to chloride (Valentine and Jafvert, 1992). A variety of intermediate species are produced throughout the breakpoint process, some of which lead to the formation of radicals and other reactive species before decaying into inorganic nitrogen including nitrate and nitrogen gas (Phillip and Diyamandoglu, 2000; Driss and Bouhelassa, 2014). Prior studies have examined the role of breakpoint chlorination in the formation of disinfection byproducts (DBPs) when organic precursors are present, including the formation of toxic nitrosamines and other DBPs (Le Roux et al., 2011; Mitch et al., 2005; Yang et al., 2005; Szczuka et al., 2020). Peroxynitrite ($ONOO^-$) and peroxynitrous acid (ONOOH) are reported to form during breakpoint chlorination. They in turn decay into reactive nitrogen species, $NO^\bullet$ and $NO_2^\bullet$ which have been implicated in the generation of nitrogenous DBPs, as well as hydroxyl radical ($HO^\bullet$) (Schreiber and Mitch, 2007).

In contrast to the findings that breakpoint chlorination can contribute to DBP formation in organics-laden water; when breakpoint chlorination takes place with only trace levels of organics present, the generation of oxidative radicals could be beneficial by oxidizing organic contaminants. This phenomenon could have major impacts on the understanding of chlorine based AOPs, but relatively little is known about the oxidative capacity of breakpoint chlorination. $HO^\bullet$ was postulated to be involved in the degradation of carbamazepine during breakpoint chlorination (Wang et al., 2018). However, the pathway of $HO^\bullet$ generation, the nature of other short-lived reactive species, and the possibility of exploiting breakpoint chlorination chemistry for rapid removal of organic contaminants remain little studied. Considering the growing interest in implementation of UV/free chlorine in treatment trains and the importance of breakpoint chlorination in water treatment, it is imperative to further investigate the radical chemistry of breakpoint chlorination.

1,4-Dioxane (1,4-D) – an organic contaminant resistant to conventional physical/chemical treatment – is ubiquitous in potable reuse scenarios. It has served as a benchmark contaminant in AOP applications, where 0.5-log-removal of 1,4-D is required to validate AOP water reuse applications in California (Advanced Treatment Criteria, 2018). A better understanding of 1,4-D oxidation during breakpoint chlorination could facilitate the optimization of chlorine-based AOPs for potable reuse and help elucidate the oxidative capacity of breakpoint chlorination. The objectives of this study were to examine the oxidative capacity of the breakpoint chlorination process with respect to degradation of 1,4-D (and organic pollutants in general) under water quality conditions relevant to water treatment, elucidate the pathway(s) of $HO^\bullet$ generation, and examine the nature of other related radical or reactive species.

2. Methods and materials

All chemicals used were ACS Reagent grade or better and purchased from Acros Organics or Fisher Scientific. Free chlorine stock solutions were freshly prepared by diluting from a commercial NaOCl stock, which was standardized using spectrophotometric permanganate reference DPD measurement (Clesceri et al., 1989). Ultrapure water (MilliQ, resistivity $\geq$ 18.1 MΩ-cm) was used to prepare all solutions. In most experiments, a 2-mM total ammonia solution was prepared using ammonium sulfate, buffered at pH 7 with 40 mM phosphate, and transferred to a 50-mL reactor for experiments in ambient air, followed by the addition of 250 μM 1,4-D. The presence of phosphate buffer had a negligible effect on radical scavenging (Patton et al., 2017). To start an experiment, 0.15–6 mM of free chlorine was rapidly injected into the reactor containing 2 mM ammonia under constant agitation with a PTFE-coated magnetic stir bar. These conditions are near typical secondary effluent ammonia concentrations (~0.1–1 mM) and applied chlorine concentrations (~0.01–0.5 mM) encountered in conventional wastewater treatment (Leong et al., 2008; Tchobanoglous et al., 2014). Additional experiments were conducted at lower reactant concentrations (36 μM ammonia, 56 μM free chlorine, and with 0.5 μM nitrobenzene as an $HO^\bullet$ probe) to approximate conditions likely to be encountered in water reuse scenarios – specifically in reverse osmosis permeate (Text S1). Prior to free chlorine addition and periodically afterward, 2-mL sample volumes were withdrawn from the reactors for free and/or total chlorine and 1,4-D or nitrobenzene analysis. Radical scavenger tests involving *tert*-butanol were performed at free chlorine-to-ammonia (Cl_2-to-NH_3) molar ratios ranging from 0.25 to 3.

To elucidate the $HO^\bullet$ formation mechanism, a 50-mL glass vessel with a ground glass stopper was used to prevent air-water exchange and evaluate the effects of dissolved CO_2 and carbonate species on behavior of $HO^\bullet$ and the $HO^\bullet$ precursor, $ONOOH/ONOO^-$. In one set of experiments undertaken at pH 7, the ammonia solution was prepared at 2 mM, buffered with 40 mM phosphate to pH 7, and dosed with 1–100 mM of freshly prepared $NaHCO_3$, followed by addition of 3 mM free chlorine. Under such conditions, ~18% of the added total carbonate ($TOTCO_3$) would have been present as H_2CO_3 * (i.e., dissolved CO_2), and ~82% as HCO_3^-. In another set of experiments undertaken at pH 4, the same solution was prepared without phosphate buffer or headspace and immediately adjusted to pH ~3.8 with $HClO_4$, followed by addition of 3 mM free chlorine. For the pH 4 experiments, the pH was initially set lower (~3.8) to account for pH increases due to addition of free chlorine (as NaOCl). Under such conditions, > 99% of $TOTCO_3$ would have been present as H_2CO_3 * /CO_2. Following free chlorine addition, the pH 4 or 7 solutions were allowed to react for 5 min, after which samples were collected and immediately quenched with sodium thiosulfate for subsequent 1,4-D analysis. In each of these experiments, pH was measured before and after free chlorine addition. Control experiments without $NaHCO_3$ amendment were also conducted at pH 4 and 7 to evaluate the effects of pH shift alone on breakpoint oxidation.

Free chlorine and chloramine concentrations in experimental samples were quantified by standard *N*,*N*-diethyl-*p*-phenylenediamine (DPD) colorimetry using a Hach DR 4000 spectrometer (Clesceri et al., 1989). The concentrations of 1,4-D and nitrobenzene were determined using an HPLC-UV system (Agilent 1200 series) as described in a prior study (Patton et al., 2018).

3. Results and discussion

3.1. Effects of chlorine-to-ammonia molar ratio on 1,4-D removal

The oxidative capacity of the breakpoint chlorination reaction was first examined as a function of the Cl_2-to-NH_3 molar ratio. When the molar ratio was less than 0.75, the percentage of 1,4-D removal after 5 min of reaction was less than 15%. The removal reached a maximum of 25% at a molar ratio of 1.5 and declined above a 2.0 molar ratio (Fig. 1). The removal of 1,4-D had a negative correlation with total chlorine residual. The highest 1,4-D removal was observed at a 1.5 molar ratio, where the lowest total chlorine was detected (Fig. S1). Further, the removal of 1,4-D was rapid, occurring within the first minute of reaction, after which the system stabilized (Fig. S2). In addition, at lower chlorine and ammonia concentrations selected to reflect potable reuse conditions, a comparable removal of nitrobenzene, a $HO^\bullet$ probe compound, was also observed at the 1.5 molar ratio (Fig. S3).

From a 0.15–1.5 Cl_2-to-NH_3 molar ratio, the reaction of ammonia with free chlorine generates mono-, di-, and trichloramine (R1 – R3 in Scheme 1; all subsequent reactions refer to Scheme 1) and is here

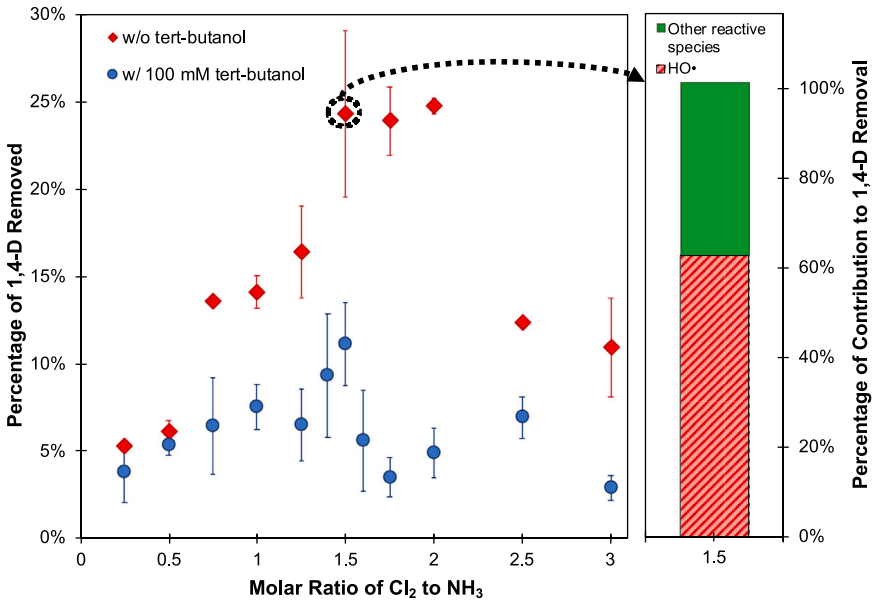

Fig. 1. The removal of 1,4-D during breakpoint chlorination at pH 7. The colored stacked bar depicts estimated contributions of $HO^{\bullet}$ and other reactive species to 1,4-D removal for the designated data point (details on calculations of contributions in SI Text S2). $[NH_3]_0 = 2$ mM, $[1,4\text{-D}]_0 = 250$ μM; $[TOTPO_4] = 40$ mM. Reaction time = 5 min.

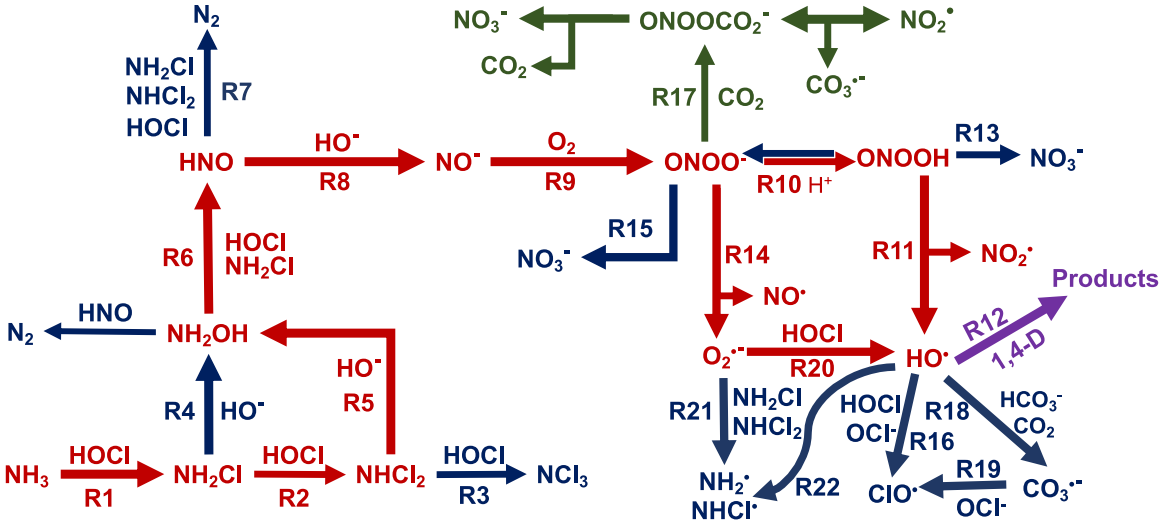

Scheme 1. Reaction scheme for the breakpoint chlorination system, with proposed pathways and major species involved in the oxidation of 1,4-D highlighted in **Red** text. (For interpretation of the references to colour in this figure legend, the reader is referred to the web version of this article.)

proposed to generate $ONOO^-$ via a hydroxylamine (NH_2OH)-initiated pathway (R4 – R9). The proposed pathway leading to $HO^{\bullet}$ formation is likely initiated by the hydrolysis of NH_2Cl and/or $NHCl_2$ to generate NH_2OH (R4-R5), with hydrolytic decay of $NHCl_2$ (R5) occurring much faster than for NH_2Cl (R4) at the pH values examined (Saunier and Selleck, 1979; Anbar and Yagil, 1962). NH_2OH may then be oxidized by NH_2Cl and HOCl to form nitroxyl (HNO) with rate constants of 1.8×10^2 and 1.35×10^7 $M^{-1}s^{-1}$, respectively (R6) (Wahman et al., 2014; Giles, 1999). Alternatively, $NHCl_2$ may hydrolyze to yield NHClOH and Cl^-, followed by elimination of HCl from NHClOH to yield HNO (Szczuka et al., 2020). HNO can react with chlorine/chloramines to generate N_2 as an end product in a side reaction (R7), but more importantly, HNO deprotonates to NO^- (R8), which reacts rapidly with oxygen to generate peroxynitrite $ONOO^-$ (R9; $k = 2.7 \times 10^9$ $M^{-1}s^{-1}$). (Shafirovich and Lymar, 2003). $ONOO^-$ can protonate to form peroxynitrous acid ONOOH with a pK_a of 6.6 (R10),(Kissner et al., 1997) which can then decay directly to $HO^{\bullet}$ and nitrogen dioxide radical $NO_2^{\bullet}$ (R11; $k = 3.5 \times 10^{-1}$ s^{-1}) (Saunier et al., 1979). This process would lead to the oxidation of 1,4-D by $HO^{\bullet}$ (R12). ONOOH can also decompose into NO_3^- (R13; $k = 9.0 \times 10^{-1}$ s^{-1}) (Saunier et al., 1979; Goldstein and Rabani, 2007). In addition, $ONOO^-$ can decompose directly into $NO^{\bullet}$ and $O_2^{\bullet-}$ (R14; $k = 2.0 \times 10^{-2}$ s^{-1}) or NO_3^- (R15; $k = 9.6 \times 10^{-6}$ s^{-1}) (Saunier et al., 1979).

As the Cl_2-to-NH_3 molar ratio increases beyond 2.0, additional reactions become significant. The reactions of NH_2Cl and $NHCl_2$ with HOCl lead to NCl_3 formation (R2-R3). Shifts in chloramine speciation toward NCl_3 would hinder R4 and R5, and increased HOCl concentrations could disrupt the oxidative pathway by competing for HNO (R7) and/or by reacting directly with $HO^{\bullet}$ (R16), while generating other less reactive secondary radicals. This could in turn lead to a decrease in removal of 1,4-D by oxidizing reactive species.

3.2. Generation of radicals and/or other reactive species

To elucidate contributions of radicals and/or other reactive species to 1,4-D removal, selective scavenging was employed to suppress contributors to 1,4-D degradation. *tert*-Butanol (TBA) was chosen as a $HO^{\bullet}$ scavenger due to its high-rate constant with $HO^{\bullet}$ (6.0×10^8 $M^{-1}s^{-1}$) (Buxton et al., 1988), and lack of reactivity toward free chlorine. In the presence of 100 mM TBA, 1,4-D removal was significantly suppressed, especially between Cl_2-to-NH_3 molar ratios of 1.5 and 2.0, where the suppression was approximately 60% (Fig. 1), consistent with the generation of $HO^{\bullet}$ in breakpoint chlorination. However, there was still substantially greater removal of 1,4-D in the presence of TBA than would be expected based on theoretical scavenging efficiency calculations (Text S2), which indicated that suppression of 1,4-D degradation should have been closer to 92% under these conditions. This points to 1,4-D degradation through additional pathways involving other reactive species that are either not scavenged or less effectively scavenged by TBA than $HO^{\bullet}$, or whose formation would not have been precluded by reaction of $HO^{\bullet}$ with TBA. This could potentially include weaker radicals such as $NO_2^{\bullet}$, which could be generated from ONOOH/$ONOO^-$ decay (see pathways R11 and R17 in Scheme 1) (Saunier et al., 1979). It could also include radicals such as $ClO^{\bullet}$ (see note in Text S2) or $NHCl^{\bullet}$, which could be generated from secondary reactions of $HO^{\bullet}$ (or $CO_3^{\bullet-}$) with matrix constituents such as HOCl/OCl^- or NH_2Cl (Remucal and Manley, 2016; Mangalgiri et al., 2019; Poskrebyshev et al., 2003a). Based on the measurements with *t*-BuOH, $HO^{\bullet}$ was estimated as contributing ~60% to 1,4-D removal under the investigated conditions (Text S2), while the remaining ~40% was tentatively attributed to "other reactive species" (right panel in Fig. 1).

The involvement of ONOOH/$ONOO^-$ in $HO^{\bullet}$ formation during breakpoint chlorination has significant implications for contaminant degradation in water treatment (Merényi et al., 1998; Merényi and Lind, 1998). However, this $HO^{\bullet}$ pathway has not been explicitly demonstrated in the context of breakpoint chlorination. To further investigate the potential role of ONOOH/$ONOO^-$ in $HO^{\bullet}$ formation, additional experiments were undertaken in which reaction solutions were amended with $NaHCO_3$ at pH 7 and 4. Amendment with $NaHCO_3$ is expected to have two primary effects under these conditions. First, $ONOO^-$ is in equilibrium with ONOOH (R10), which decays directly into $HO^{\bullet}$ and $NO_2^{\bullet}$ (R11). H_2CO_3 * /CO_2 and HCO_3^- can react with $HO^{\bullet}$ (e.g., R18; $k < 10^6$ $M^{-1}s^{-1}$ for H_2CO_3 */CO_2 and $k = 8.5 \times 10^6$ $M^{-1}s^{-1}$ for HCO_3^-)(Keene and Raef, 1965; Buxton et al., 1988) to produce $CO_3^{\bullet-}$. As $TOTCO_3$ (and H_2CO_3 */CO_2 and HCO_3^-) concentration increases, the branching ratio between R12 and R18 is therefore expected to shift towards R18 and increased formation of $CO_3^{\bullet-}$. Second, $ONOO^-$ is reported to react rapidly with dissolved CO_2 to form $ONOOCO_2^-$ (R17; $k = 2.9 \times 10^4$ $M^{-1}s^{-1}$) (Saunier et al., 1979). $ONOOCO_2^-$ can then decay into $CO_3^{\bullet-}$ and $NO_2^{\bullet}$, or CO_2 and NO_3^-. (Lymar and Hurst, 1998). As $TOTCO_3$ (and dissolved CO_2) concentration increases, the branching ratio between R11 and R17 is therefore also anticipated to shift towards R17 (Fig. S5A). This would suppress the formation of $HO^{\bullet}$ via R11, but still ultimately favor the generation of $CO_3^{\bullet-}$. As noted above, $NO_2^{\bullet}$ will also be generated in parallel with $CO_3^{\bullet-}$ in each of these cases. $CO_3^{\bullet-}$ itself is anticipated to have a relatively low reactivity toward 1,4-D based on its reactions with other structurally-similar compounds (e.g., k~10^5 $M^{-1}s^{-1}$ with the structurally similar tetrahydrofuran). (Neta et al., 1988; Wojnárovits et al., 2020; Clifton and Huie, 1993). By analogy, $NO_2^{\bullet}$ – which is a weaker oxidant than $CO_3^{\bullet-}$ – is also expected to have a comparatively low reactivity toward 1,4-D. (Neta et al., 1988).

Results showed that the presence of 1 mM $TOTCO_3$ at pH 4 (comprising >99% H_2CO_3 */CO_2) lowered the overall removal of 1,4-D by 40%, while the same concentration of $TOTCO_3$ at pH 7 (comprising ~18% H_2CO_3 */CO_2 and ~82% HCO_3^-) lowered the removal by less than 2% (Fig. 2). Increasing $TOTCO_3$ from 1 to 5 mM at pH 4 resulted in a 70% decrease in 1,4-D removal, whereas addition of 10 mM $TOTCO_3$ at pH 4 resulted in complete suppression of 1,4-D removal. In contrast, the addition of $TOTCO_3$ concentrations up to 100 mM at pH 7 resulted in an 80% decrease in 1,4-D removal (Fig. 2).

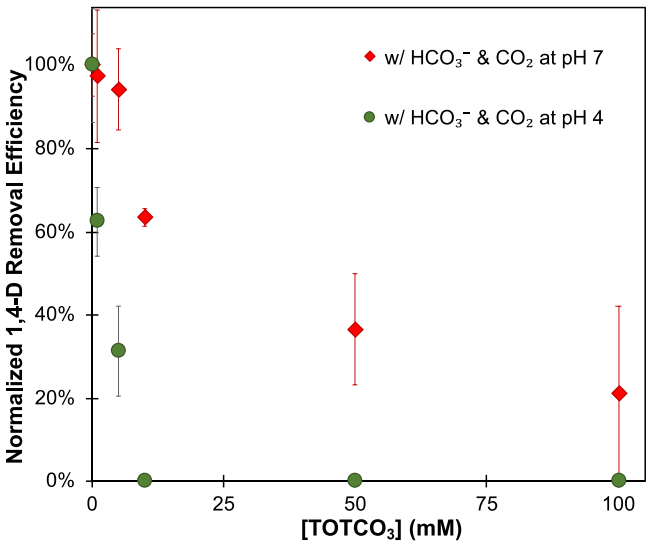

Fig. 2. The impact of increasing concentrations of added HCO_3^- on 1,4-D removal efficiency at pH 7 and 4. Normalized removal efficiencies are the removals of 1,4-D normalized to removals observed for added $[HCO_3^-] = 0$ mM (i.e., $[TOTCO_3] = 0$ mM in the figure) at either pH 7 (red symbols) or pH 4 (green symbols), to enable comparison of the two datasets independent of the impact of pH (see Fig. S5B for data without normalization). pH 7 was maintained by 40 mM phosphate buffer, whereas pH 4 was achieved with $HClO_4$ titration prior to experiments. $[1,4\text{-D}]_0 = 250$ μM, $[NH_3]_0 = 2$ mM, $[HOCl]_0 = 3$ mM. Reaction time = 5 min. (For interpretation of the references to colour in this figure legend, the reader is referred to the web version of this article.)

The predicted decreases in % 1,4-D removal due to R18 at both pH 4 and 7 are negligible in comparison to the measured decreases in % 1,4-D removal at each pH over increasing $TOTCO_3$ concentrations (Text S3, Fig. S5B), indicating that the impact of $TOTCO_3$ addition is not due to scavenging of $HO^{\bullet}$ by carbonate species, and is rather attributable to sequestration of ONOOH/$ONOO^-$ by dissolved CO_2 present in equilibrium with carbonate species (R17) – leading to decreased formation of $HO^{\bullet}$ via decay of ONOOH/$ONOO^-$ (R11). This is further supported by the generally good agreement of measured decreases in 1,4-D removal at pH 4 with those predicted at the same pH based on R17 branching ratios (Text S3, Fig. S5B).

However, it is also important to note that at pH 7, the experimentally observed attenuation of 1,4-D removal by $TOTCO_3$ addition is significantly less than that predicted from calculated branching ratios for R17 (Fig. S5B). This may be due in part to uncertainties in the kinetics or yields of the CO_2 reaction with ONOOH/$ONOO^-$ at elevated $TOTCO_3$ concentrations (Koppenol et al., 2020). It is also possible that $CO_3^{\bullet-}$ (or perhaps also $NO_2^{\bullet}$) generated via the reaction between $ONOO^-$ and CO_2 could further react with OCl^- and NH_2Cl to generate $ClO^{\bullet}$ (R19) and $NHCl^{\bullet}$ (or other chloramine radicals), (Clifton and Huie, 1993; Poskrebyshev et al., 2003b; Wojnárovits et al., 2020) respectively, which – even if not directly reactive toward 1,4-D (see note in Text S2) – may themselves drive secondary reactions involving other as yet unidentified reactive species. It is especially worth noting that reaction of $CO_3^{\bullet-}$ with HOCl is likely to be quite slow based on the reported rate constant for reaction of $CO_3^{\bullet-}$ with OCl^- (i.e., k ~ 5–6 × 10^5 $M^{-1}s^{-1}$), (Alfassi et al., 1988; Huie et al., 1991; Clifton and Huie, 1993; Wojnárovits et al., 2020) recognizing that protonated acid-base species are typically considerably less reactive toward oxidants than their deprotonated conjugates (Stumm and Morgan, 1995). If $ClO^{\bullet}$ is an important driver of further reactions involving 1,4-D in these systems, this could provide one potential explanation for the apparently good agreement between measured and predicted 1,4-D removal based on R17 at pH 4, and the

correspondingly poor agreement between measurements and predictions based on R17 at pH 7, as $ClO^{\bullet}$ formation would likely be much less significant at pH 4 due to the dominance of HOCl versus OCl^{-} ($\alpha_{HOCl} \sim 1$ vs. $\alpha_{OCl^-} = 3.2 \times 10^{-4}$) in comparison to pH 7 ($\alpha_{HOCl} \sim 0.76$ vs. $\alpha_{OCl^-} = 0.24$). That is, the much lower than predicted attenuation of 1,4-D degradation (i.e., the higher than predicted degradation of 1,4-D) at pH 7 might reflect a role of $ClO^{\bullet}$ as a progenitor of secondary species that could serve as direct oxidants of 1,4-D. In light of the preceding, future research into the potential roles of $CO_3^{\bullet-}$, $NO_2^{\bullet}$, and $ClO^{\bullet}$ as drivers of breakpoint chemistry (as well as the potential role(s) of chloramine radical(s)) is highly encouraged.

Notably, the decrease in pH from 7 to 4 also lowers 1,4-D removal in the absence of carbonate species, though to a lesser degree than observed in the presence of carbonate species (Fig. S5B). The pH effect may be due to a suppression of OH^{-}-driven NH_2Cl and $NHCl_2$ hydrolysis (R4, R5) at lower pH, consistent with the proposed role of chloramine hydrolysis in breakpoint-based oxidation (Saunier et al., 1979). Alternatively (or perhaps additionally), the pH effect could reflect a role for the reaction of $O_2^{\bullet-}$ (generated in R14) with HOCl to yield $HO^{\bullet}$ (R20; $k = 7.5 \times 10^6\ M^{-1}s^{-1}$) (Long and Bielski, 1980), since protonation of $ONOO^{-}$ at pH < $pK_{a,ONOOH}$ (= 6.6) would also be expected to diminish the importance of such a reaction. In addition, $O_2^{\bullet-}$ could react with $NH_2Cl/NHCl_2$ to yield $NH_2^{\bullet}/NHCl^{\bullet}$ (R21), based on similar reactions between $O_2^{\bullet-}$ and organic chloramines (Pattison et al., 2002; Parsons et al., 2013; Hawkins et al., 2002; Rees et al., 2004; Rees and Davies, 2006). In either case, the above findings suggest that $ONOOH/ONOO^{-}$ is a primary driver of 1,4-D removal by $HO^{\bullet}$ (and potentially other secondary radical species) in the breakpoint chlorination system.

4. Conclusions

This study advances the understanding of breakpoint chlorination processes by elucidating likely pathways for the generation of $HO^{\bullet}$ and related reactive species and evaluating their direct contributions to the degradation of an important trace organic contaminant. Significant $HO^{\bullet}$ exposures (up to $\sim 2 \times 10^{-10}$ M•s, Fig. 3 and S3) were observed during breakpoint chlorination under the conditions investigated here, placing it on par with many UV-AOPs as an oxidative process that operates within a relatively short reaction time, but without the use of UV light. This process was shown to operate both at relatively high reactant concentrations approximating wastewater treatment (Figs. 1 and 3), as well as under lower reactant concentration conditions more representative of water reuse – in a matrix approximating reverse osmosis permeate (Text S1, Fig. S3). The identification of $ONOOH/ONOO^{-}$ as a likely driver of breakpoint oxidation warrants future work in exploring this process and its complex role in water treatment.

For example, these findings suggest probable avenues for further enhancement of organic contaminant degradation during the breakpoint chlorination process. $ONOO^{-}$ has high molar absorption coefficients of 550 $M^{-1}cm^{-1}$ and 1700 $M^{-1}cm^{-1}$ at 254 nm and 302 nm, respectively, and may photolyze to generate reactive oxygen and nitrogen species (Bohle et al., 1994; Goldstein and Rabani 2007). These high molar absorption coefficients, coupled with the accompanying susceptibility to photolysis of chloramines and free chlorine, imply that the simultaneous photolysis of a solution undergoing breakpoint chlorination may enable more effective oxidation than breakpoint chlorination alone. However, the generation of $HO^{\bullet}$ during breakpoint chlorination may also lead to the formation of unexpected DBPs, as organics may be hydroxylated or fragmented via $HO^{\bullet}$ oxidation and then chlorinated (Ike et al., 2019; Ike et al., 2019). Further, the presence of reactive nitrogen species may lead to nitrogenous DBPs such as chloropicrin and *N*-nitrosodimethylamine, which may further complicate DBP formation risk models (Schreiber and Mitch 2007; Scholes et al., 2019; Shah et al., 2011; Szczuka et al., 2020).

These findings highlight newly recognized aspects of breakpoint chlorination chemistry that are important regarding existing treatment methods, and that may also be exploited for existing and new AOPs; potentially enhancing the efficiency of water treatment processes and expanding the range of possible potable water supplies, though with need for caution on account of the potential for accompanying enhancement of disinfection byproduct formation under such conditions.

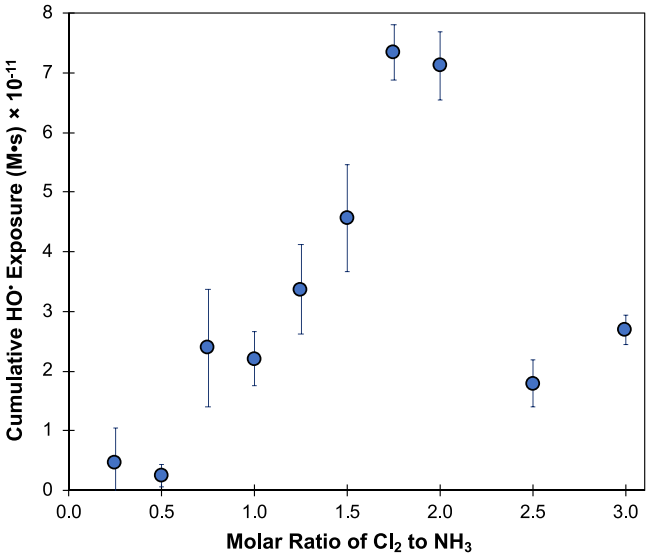

Fig. 3. Cumulative $HO^{\bullet}$ exposures calculated based on *tert*-butanol experiments. $[NH_3]_0 = 2$ mM, $[1,4\text{-D}]_0 = 250$ μM; [*tert*-butanol]= 100 mM; $[TOTPO_4] = 40$ mM. Reaction time = 5 min. Details of the calculations are available in SI Text S2.

Funding information

This work was supported by grants to H.L. from National Science Foundation (CBET-1653931,CHE-1611306 and CHE-1808242) and to S. P. from the National Science Foundation Graduate Research Fellowship and IGERT Water Sense Fellowship. M.C.D gratefully acknowledges support from the Allan & Inger Osberg Endowed Professorship.

Declaration of Competing Interest

The authors declare that they have no known competing financial interests or personal relationships that could have appeared to influence the work reported in this paper.

Acknowledgments

This work was supported by grants to H.L. from National Science Foundation (CBET-1653931, CHE-1611306 and CHE-1808242) and to S.P. from the National Science Foundation Graduate Research Fellowship and IGERT Water Sense Fellowship. M.C.D gratefully acknowledges support from the Allan & Inger Osberg Endowed Professorship. We are grateful for the assistance and feedback provided by the H. Liu group members and Ken Ishida at Orange County Water District.

Appendix A. Supporting information

Additional texts on experimental details, radical reaction calculations, and figures on radical exposure and branching ratio calculations are provided in the Supplementary Information. Supplementary data associated with this article can be found in the online version at doi:10.1016/j.hazl.2022.100054.

References

Advanced Treatment Criteria. California Department of Public Health Regulations Related to Recycled Water; California Department of Public Health: Sacramento, CA, 2018; Section 60320.201, Title 22.

Alfassi, Z.B., Huie, R.E., Mosseri, S., Neta, P., 1988. Kinetics of one-electron oxidation by the ClO radical. Int. J. Rad. Appl. Instrum. Part C Rad. Phys. Chem. 32 (1), 85–88.

Anbar, M., Yagil, G., 1962. The hydrolysis of chloramine in alkaline solution. J. Am. Chem. Soc. *84* (10), 1790–1796.

Bohle, D.S., Hansen, B., Paulson, S.C., Smith, B.D., 1994. Biomimetic synthesis of the putative cytotoxin peroxynitrite, ONOO-, and its characterization as a tetramethylammonium salt. J. Am. Chem. Soc. 116 (16), 7423–7424.

Buxton, G.V., Greenstock, C.L., Helman, W.P., Ross, A.B., 1988. Critical review of rate constants for reactions of hydrated electrons, hydrogen atoms and hydroxyl radicals (•OH/•O-) in Aqueous Solution. J. Phys. Chem. Ref. Data 17 (2), 513–886.

Clesceri, L. S.; Greenberg, S. E.; Trussell, R. R. Standard Methods for the Examination of Water and Wastewater, 17th ed.; American Public Health Association: Washington, DC, 1989.

Clifton, C.L., Huie, R.E., 1993. Rate constants for some hydrogen abstraction reactions of the carbonate radical. Int. J. Chem. Kinet. 25 (3), 199–203.

Driss, K., Bouhelassa, M., 2014. Modeling drinking water chlorination at the breakpoint: I. Derivation of breakpoint reactions. Desalin. Water Treat. *52* (31–33), 5757–5768.

Duan, X., Sanan, T., De La Cruz, A., He, X., Kong, M., Dionysiou, D.D., 2018. Susceptibility of the algal toxin microcystin-LR to UV/chlorine process: comparison with chlorination. Environ. Sci. Technol. 52 (15), 8252–8262.

Giles, B., 1999. Thesis: The Oxidation Of Hydroxylamine By Hypohalites And Other Halogen Containing Species. Purdue University.

Saunier, B.M., Selleck, R.E., 1979. Kinetics of breakpoint chlorination in continuous flow systems. J. Am. Water Work. Assoc. 71 (3), 164–172.

Goldstein, S., Rabani, J., 2007. Mech nitrite formation by nitrate photolysis in aq solns: role of peroxynitrite, nitrogen dioxide no2, hydroxyl radical. J. Am. Chem. Soc. 129 (34), 10597–10601.

Goldstein, S., Rabani, J., 2007. Mechanism of nitrite formation by nitrate photolysis in aqueous solutions: the role of peroxynitrite, nitrogen dioxide NO2, hydroxyl radical. J. Am. Chem. Soc. 129 (34), 10597–10601.

Hawkins, C.L., Rees, M.D., Davies, M.J., 2002. Superoxide radicals can act synergistically with hypochlorite to induce damage to proteins. FEBS Lett. 510, 41–44.

Huie, R.E., Clifton, C.L., Neta, P., 1991. Electron transfer reaction rates and equilibria of the carbonate and sulfate radical anions. Radiat. Phys. Chem. *38* (5), 477–481.

Ike, I.A., Karanfil, T., Cho, J., Hur, J., 2019. Oxidation byproducts from the degradation of dissolved organic matter by advanced oxidation processes – a critical review. Water Res. 164, 114929.

Ike, I.A., Lee, Y., Hur, J., 2019. Impacts of advanced oxidation processes on disinfection byproducts from dissolved organic matter upon post-chlor(am)ination: a critical review. Chem. Eng. J. 375, 121929.

Keene, J.P., Raef, Y., Swallow, A.J., 1965. Pulse radiolysis studies of carboxyl and related radicals. In: Ebert, M., Keene, J.P., Swallow, A.J., Baxendale, J.H. (Eds.), Pulse Radiolysis. Academic Press, New York, pp. 99–106.

Kissner, R., Nauser, T., Bugnon, P., Lye, P.G., Koppenol, W.H., 1997. Formation and properties of peroxynitrite as studied by laser flash photolysis, high-pressure stopped-flow technique, pulse radiolysis. Chem. Res. Toxicol. *10* (11), 1285–1292.

Koppenol, W.H., Serrano-Luginbuehl, S., Nauser, T., Kissner, R., 2020. Thinking outside the cage: a new hypothesis that accounts for variable yields of radicals from the reaction of CO with $ONOO^-$. Chem. Res. Toxicol. 33 (7), 1516–1527.

Leong, L.Y.C., Kuo, J. and Tang, C.-C., Disinfection of Wastewater Effluent - Comparison of Alternative Technologies (2008) Water Environment Research Foundation Alexandria, VA.

Long, C.A., Bielski, B.H.J., 1980. Rate of reaction of superoxide radical with chloride-containing species. J. Phys. Chem. 84 (5), 555–557.

Lymar, S.V., Hurst, J.K., 1998. CO 2 -catalyzed one-electron oxidations by peroxynitrite: properties of the reactive intermediate. Inorg. Chem. 37 (2), 294–301.

Mangalgiri, K.P., Patton, S., Wu, L., Xu, S., Ishida, K.P., Liu, H., 2019. Optimizing potable water reuse systems: chloramines or hydrogen peroxide for UV-based advanced oxidation process? Environ. Sci. Technol. 53 (22), 13323–13331.

Merényi, G., Lind, J., Goldstein, S., Czapski, G., 1998. Peroxynitrous acid homolyzes into $^{\bullet}OH$ and $^{\bullet}NO_2$ radicals. Chem. Res. Toxicol. *11* (7), 712–713.

Merényi, G., Lind, J., 1998. Free radical formation in the peroxynitrous acid (ONOOH)/peroxynitrite (ONOO-) system. Chem. Res. Toxicol. *11* (4), 245–246.

Mitch, W.A., Oelker, G.L., Hawley, E.L., Deeb, R.A., Sedlak, D.L., 2005. Minimization of NDMA formation during chlorine disinfection of municipal wastewater by application. Environ. Eng. Sci. 22 (6), 882–891.

Neta, P., Huie, R.E., Ross, A.B., 1988. Rate constants for reactions of inorganic radicals in aqueous solution. J. Phys. Chem. Ref. Data 17 (3), 1027–1284.

Neta, P., Huie, R.E., Ross, A.B., 1988. Rate constants for reactions of inorganic radicals in aqueous solution. J. Phys. Chem. Ref. Data 17 (3), 1027–1284.

Parsons, B.J., Sibanda, S., Heyes, D.J., Paterson, A.W.J., 2013. Reaction of superoxide radicals with glycosaminoglycan chloramides: a kinetic study. Free Rad. Biol. Med. 61, 111–118.

Pattison, D., Davies, I., Asmus, M.J., A, K.-D., 2002. Absolute rate constants for the formation of nitrogen-centred radicals from chloramines/amides and their reactions with antioxidants. J. Chem. Soc., Perkin Trans 2, 1461–1467.

Patton, S., Li, W., Couch, K.D., Mezyk, S.P., Ishida, K.P., Liu, H., 2017. Impact of the ultraviolet photolysis of monochloramine on 1,4-dioxane removal: New insights into potable water reuse. Environ. Sci. Technol. Lett. 4, 1.

Patton, S., Romano, M., Naddeo, V., Ishida, K.P., Liu, H., 2018. Photolysis of mono- and di-chloramines in UV/hydrogen peroxide: effects on 1,4-dioxane removal and relevance in water reuse. Environ. Sci. Technol.

Phillip, N., Diyamandoglu, V., 2000. Kinetics of nitrate formation in breakpoint chlorination. Proc. Water Environ. Fed 2000 (2), 145–152.

Poskrebyshev, G.A., Huie, R.E., Neta, P., 2003a. Radiolytic reactions of monochloramine in aqueous solutions. Journal of Physical Chemistry, A *107* (38), 7423–7428.

Poskrebyshev, G.A., Huie, R.E., Neta, P., 2003b. Radiolytic reactions of monochloramine in aqueous solutions. Journal of Physical Chemistry, A *107* (38), 7423–7428.

Rees, M.D., Davies, M.J., 2006. Heparan sulfate degradation via reductive homolysis of its N-chloro derivatives. J. Am. Chem. Soc. 128, 3085–3097.

Rees, M.D., Hawkins, C.L., Davies, M.J., 2004. Hypochlorite and superoxide radicals can act synergistically to induce fragmentation of hyaluronan and chondroitin sulphates. Biochem. J. 381, 175–184.

Remucal, C.K., Manley, D., 2016. Emerging investigators series: the efficacy of chlorine photolysis as an advanced oxidation process for drinking water treatment. Environ. Sci. Water Res. Technol *2* (4), 565–579.

Le Roux, J., Gallard, H., Croué, J.P., 2011. Chloramination of nitrogenous contaminants (pharmaceuticals and pesticides): NDMA and halogenated DBPs formation. Water Res. 45 (10), 3164–3174.

Saunier, B.M., Selleck, R.E., 1979. Kinetics of breakpoint chlorination in continuous flow systems. J. Am. Water Work. Assoc. 71 (3), 164–172.

Scholes, R.C., Prasse, C., Sedlak, D.L., 2019. The role of reactive nitrogen species in sensitized photolysis of wastewater-derived trace organic contaminants. Environ. Sci. Technol. 53 (11), 6483–6491.

Schreiber, I.M., Mitch, W.A., 2007. Enhanced nitrogenous disinfection byproduct formation near the breakpoint: Implications for nitrification control. Environ. Sci. Technol. *41* (20), 7039–7046.

Shafirovich, V., Lymar, S.V., 2003. Spin-forbidden deprotonation of aqueous nitroxyl (HNO). J. Am. Chem. Soc. *125* (21), 6547–6552.

Shah, A.D., Dotson, A.D., Linden, K.G., Mitch, W.A., 2011. Impact of UV disinfection combined with chlorination/chloramination on the formation of halonitromethanes and haloacetonitriles in drinking water. Environ. Sci. Technol. 45, 3657–3664.

Stumm, W.; Morgan, J. J. *Aquatic Chemistry: Chemical Equilibria and Rates in Natural Waters*, 3rd Edition. 1995. John Wiley & Sons, INC. New York.

Szczuka, A., Huang, N., Macdonald, J.A., Nayak, A., Zhang, Z., Mitch, W.A., 2020. N-nitrosodimethylamine formation during UV/Hydrogen peroxide and UV/chlorine advanced oxidation process treatment following reverse osmosis for potable reuse. Environ. Sci. Technol. 54 (23), 15465–15475.

Tchobanoglous, G., Stensel, H.D., Tsuchihashi, R. and Burton, F. (2014) Wastewater Engineering: Treatment and Resource Recovery, McGraw-Hill.

Valentine, R.L., Jafvert, C.T., 1992. Reaction scheme for the chlorination of ammoniacal water. Environ. Sci. Technol. 26 (3), 713–722.

Vikesland, P.J., Ozekin, K., Valentine, R.L., 2001. Monochloramine decay in model and distribution system waters. Water Res. 35 (7), 1766–1776.

Wahman, D.G., Speitel, G.E., Machavaram, M.V., 2014. A proposed abiotic reaction scheme for hydroxylamine and monochloramine under chloramination relevant drinking water conditions. Water Res. 60, 218–227.

Wang, W.L., Wu, Q.Y., Du, Y., Huang, N., Hu, H.Y., 2018. Elimination of chlorine-refractory carbamazepine by breakpoint chlorination: Reactive species and oxidation byproducts. Water Res. 129, 115–122.

Wojnárovits, L., Tóth, T., Takács, E., 2020. Rate constants of carbonate radical anion reactions with molecules of environmental interest in aqueous solution: a review. Sci. Total Environ. 717.

Yang, X., Shang, C., Huang, J.C., 2005. DBP formation in breakpoint chlorination of wastewater. Water Res. 39 (19), 4755–4767.

Zhang, R., Meng, T., Huang, C.H., Ben, W., Yao, H., Liu, R., Sun, P., 2018. PPCP degradation by chlorine-UV processes in ammoniacal water: new reaction insights, kinetic modeling, and DBP formation. Environ. Sci. Technol. 52 (14), 7833–7841.